Induced Perturbation Network and tiling for modeling the L55P Transthyretin amyloid fiber

Lorenza Pacini, Laurent Vuillon, Claire Lesieur

Available online at www.sciencedirect.com

ScienceDirect

Procedia Computer Science 178 (2020) 8–17

Procedia Computer Science

www.elsevier.com/locate/procedia

9th International Young Scientist Conference on Computational Science (YSC 2020)

Induced Perturbation Network and tiling for modeling the L55P Transthyretin amyloid fiber

Lorenza Pacini[a,b,*], Laurent Vuillon[c], Claire Lesieur[a,b]

[a] *AMPERE, CNRS, Univ. Lyon, 69622, Lyon, France*
[b] *Institut Rhônalpin des systèmes complexes, IXXI-ENS-Lyon, 69007, Lyon, France*
[c] *LAMA, Univ. Savoie Mont Blanc, CNRS, LAMA, 73376 Le Bourget du Lac, France*

Abstract

Protein structures are complex spatial systems, formed by the three-dimensional arrangement of amino acids, that interact through atomic contacts. It is fundamental to understand the perturbation mechanisms associated with the amino acid mutations that lead to changes in a protein dynamics, as such mutations can lead to diseases. We present a methodology based on Amino Acid Networks and the use of Induced Perturbation Networks to infer the impact of amino acid mutations on a protein's dynamics and the use of a tiling formalism to model protein aggregation. We apply this methodology to the case study of the L55P Transthyretin (TTR) variant, one of the most pathogenic mutations of TTR, due to its increased tendency to aggregate into amyloid fibers. We show that another pathogenic variant, V30M TTR, produces different results, reflecting a different pathogenic mechanism compared to L55P TTR and that the results differ for pathogenic and non-pathogenic variants (L55P and V30M TTR pathogenic variants versus T119Y and T119M non-pathogenic variants).

Keywords: complex system; spatial network; protein structure; protein dynamics; Amino Acid Network; Perturbation Network; Transthyretin; amyloid;

1. Introduction

Proteins are complex spatial systems, whose three-dimensional structure is built by a network of amino acids whose atoms interact through chemical bonds. According to the sequence-structure-dynamics-function paradigm, the protein function results from the dynamics of its atoms, that are controlled by their structural position and by the existing atomic interactions, in turn encoded in the protein amino acid sequence, i.e. the chain of covalently-bound amino acids by which the protein is built [1]. As an example of protein dynamics, perfringolysis O (PFO) is a protein toxin

* Corresponding author.
E-mail address: lorenza.pacini@ens-lyon.fr

1877-0509
10.1016/j.procs.2020.11.002

that, when close to the cell membrane of its host, performs major but well-controlled structural rearrangements that initiate oligomerization (*i.e.* assembly of multiple copies of the proteins) and the insertion into the cell membrane, impossible when PFO is in its initial shape [2]. The PFO example shows how the function of a protein relies on both the atomic structure and the atomic dynamics in a inter-dependent way: the atomic structure defines what atomic motions can take place, and the atomic motions yield shape changes, essential for the protein function. The complexity of proteins is evident from their multi-scale dynamics, ranging from local atomic motions to global motions involving the entire protein, controlled by signal propagation within the amino acid network.

Most amino acids in a protein can be substituted by an amino acid of different type, resulting in a functional protein variant [3]: that means that the network of atomic interactions of the protein structure is resilient to local perturbations. However, there exist cases of amino acid variants that result in a change or loss of the protein function [4]. While on the one hand the possibility of modulating the function through mutations is essential for adaptation, on the other hand, the loss of protein function or the change of its original behavior can cause diseases. Amino acid mutations can cause diseases due to several reasons [5]. In this study, we focus on amino acid mutations that impact the protein dynamics and result in the formation of toxic aggregates [6] for the case of the Transthyretin (TTR) protein, a tetrameric protein involved in neurological and cardiac genetic diseases due to the formation of amyloid fibrils aggregates [7, 8]. The wild-type (WT) TTR has an intrinsic tendency to generate amyloids, causing the Senile Systemic Amylodosis. A large set of TTR pathogenic and non-pathogenic variants are known. The pathogenic variants show an increased tendency to the formation of amyloids, causing the hereditary diseases of Familial Amyloidoic Polyneuropathy and Familial Cardiomyopathy [7, 8, 9]. Pathogenic TTR variants fall in the category of protein variants that do not impact the protein structure formation, but have an impact on the dynamics, leading to formation of amyloid aggregates. The molecular mechanisms underlying the process of amyloid formation of TTR are yet to be understood and probably depend on the particular TTR variant and on the experimental conditions [10, 11, 12, 13, 14, 15].

The amyloid fiber structure of a protein can be seen as a result of a tiling process where a repeating unit interacts with N copies of itself using one or more interfaces. The position of the interface(s) in the repeating unit will determine the growth direction of the amyloid. As a result, no matter the exact molecular mechanisms creating the repeating unit, the process of amyloid formation can be seen as a transition from the initial oligomeric state according to the following steps [16]: (i) Rearrangement of the native oligomeric structure (with or without dissociation of the oligomer); (ii) Exposure of a novel interacting interface; (iii) Eventually, formation of an asymmetric repeating unit through the interaction via the novel interface; (iv) Growth of the amyloid by successive interactions of repeating units through the novel interacting interface.

Measuring the impact of single amino acid mutations on the protein dynamics, as for the case of the amyoidogenic TTR variants, is extremely challenging, because it requires describing collective large-scale motions (slow motions) with atomistic resolution. Molecular Dynamics provide simulations of protein dynamics with atomic resolution, but are limited in terms of protein size and of temporal simulation window [17, 18]. Based on the atomic structure of proteins, Amino Acid Networks (AANs) and Perturbation Networks (PNs) have been proven successful in investigating protein dynamics and robustness to mutations [19, 20, 21]. Even though AANs do not describe the protein dynamics, the PN is employed to infer differences in dynamics among structurally equivalent protein variants based on the observation that atomic motions correspond to changes in link weights.

We used AANs, PNs and Induced Perturbation Networks (IPNs, see Methods), coupled to geometrical considerations over the TTR structure, to infer candidate interaction interfaces and models of construction of the amyloid fiber for the pathogenic L55P TTR variant, based on the sole knowledge of the crystalline structures of the WT TTR and of the variant. We validated the method by comparing the IPN of L55P TTR with the IPNs of a different pathogenic variant (V30M TTR) and two non-pathogenic variants (T119Y and T119M TTR).

2. Data

The following protein structures were downloaded from the Protein Data Bank (PDB) (`http://www.rcsb.org/`): WT TTR (PDB id: 1f41), L55P TTR (PDB id: 3djz, pathogenic variant), V30M TTR (PDB id: 3kgs, pathogenic variant), T119Y TTR (PDB id: 4tne, non-pathogenic variant) and T119M TTR (PDB id: 1bze, non-pathogenic variant). All structures contain a TTR dimer (chain A and chain B). Residues from position 11 to position 124 in the sequence

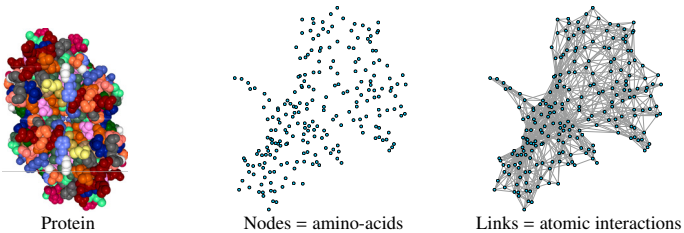

Fig. 1: Amino Acids Network (AAN) of the human wild-type Transthyretin dimer (PDB id: 1f41). *Left*: the protein structure, where the atoms are represented as spheres and colored according to the amino acid they belong to. *Center*: nodes of the AAN, corresponding to the protein amino acids. *Right:* links of the AAN, connecting amino acids that have at least two atoms at distance ≤ 5Å and weighted according to the number of atomic couples at distance ≤ 5Å.

have been considered for the analysis, both for chain A and chain B. The tetrameric structure of TTR is recovered from the assembly of two dimers reported in the PDB.

3. Methods

3.1. Amino Acid Network

Each protein structure is analyzed thanks to the construction of its Amino Acid Network (AAN) [20], represented by a weighted graph $G = (V, E, W)$ with nodes $V = \{i \mid i \text{ is an amino-acid}\}$, links $E = \{(i, j) \mid i, j \in V \text{ and } \exists\ (\text{atom}_i \in i, \text{atom}_j \in j) \text{ with } \text{dist}(\text{atom}_i, \text{atom}_j) \leq 5\text{Å}\}$ and link weights $w_{ij} \in W$ defined as the number of atomic pairs $(\text{atom}_i \in i, \text{atom}_j \in j)$ that satisfy $\text{dist}(\text{atom}_i, \text{atom}_j) \leq 5$Å. An example of AAN is reported in Fig. 1. AANs have been produced with the Python module Biographs, available at `https://github.com/rodogi/biographs` and plotted with the Python library NetworkX [22].

In the AAN, the node degree k_i is defined as the number of neighbors of a node i, the node weight w_i is defined as the sum over all the weights of the links that connect the node i to its neighbors ($w_i = \sum_{j \in N(i)} w_{ij}$, with $N(i)$ the set of neighbors of node i), and the node's Neighborhood watch Nw_i is defined as the ratio between the node's weight and the node degree ($Nw_i = w_i/k_i$), representing the average weight of interaction that a node performs with its neighbors. Different TTR variant structures have been compared through the analysis of their node properties (degree k, weight w and Neighborhood watch Nw) along the amino acids sequence.

3.2. Perturbation Network

The amino acids interactions within a protein variant (var) and the wild-type (WT) are compared through the analysis of the Perturbation Network (PN) of threshold $\bar{w}$ [21], represented by a graph $G_p = (V_p, E_p, W_p)$ with links $E_p = \{(i, j) \in E_{WT} \cup E_{var} \text{ s.t. } |w_{var}(i, j) - w_{WT}(i, j)| > \bar{w}\}$, link weights $w_p(i, j) \in W_p$ with $w_p(i, j) = |\Delta w(i, j)| = |w_{var}(i, j) - w_{WT}(i, j)|$ and link color

$$color(i, j) = \begin{cases} \text{red if } w_{var}(i, j) - w_{WT}(i, j) < -\bar{w} \\ \text{green if } w_{var}(i, j) - w_{WT}(i, j) > \bar{w} \end{cases}.$$

The set of nodes V_p is a subset of V, including all nodes for which at least one link has different weight in the variant's AAN compared to the WT AAN (*i.e.* nodes with degree zero are removed from the PN). We refer to the nodes in V_p as *perturbed nodes*. Figure 2 (third panel from the left) shows a toy example of PN.

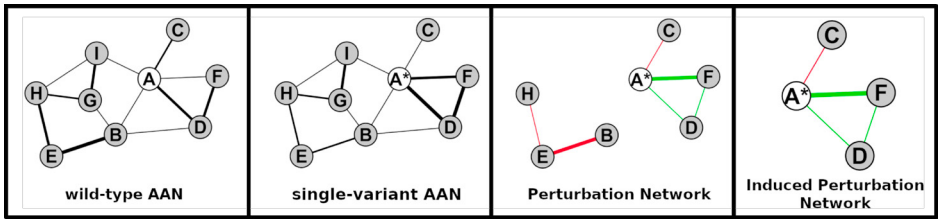

Fig. 2: Perturbation Network and Induced Perturbation Network of a toy example. From left to right: Amino Acid Network of the wild-type protein; Amino Acid Network of the variant (with single mutation from A to A*); Perturbation Network of the variant; Induced Perturbation Network of the variant. The graphs have been reproduced with the Gephi software [23].

3.3. Induced Perturbation Network

The Induced Perturbation Network (IPN) of a variant is the connected component of the PN that contains the mutation site. With respect to the PN, the construction of the IPN of a mutation allows to maintain only the information on the perturbations that have propagated from the mutation point to other areas of the protein structure. As a first approximation, the other perturbations, not connected to the mutation point, are here considered to be uncorrelated with the mutation, reflecting alternative atomic arrangements that the protein adopts when crystallized. As a result, the IPN represents the network of changes it atomic contacts in the protein structure that have been caused in the protein structure by the single mutation. Figure 2 (right-most panel) shows a toy example of IPN. The IPNs of TTR variants were used to infer candidate new interaction interfaces. This was done by identifying groups of residues that lost atomic interactions due to the mutation (red links in the IPN) and that may be responsible for the creation of a novel interface to restore their original connectivity features. We assume that the loss of atomic interactions leads to increased freedom of motion.

3.4. Choice of the perturbation threshold $\bar{w}$

The choice of the threshold $\bar{w}$ impacts the number of nodes and links in the PN and in the IPN. A low $\bar{w}$ allows capturing more differences in atomic interactions between the variant's and the WT protein structures. This is desirable to assess the highest number of perturbed nodes, that is the set of amino acids that have undergone a change in atomic interactions, but it also increases the likelihood of detecting differences corresponding to the reproduction of alternative solutions for atomic interactions that do not correspond to a rearrangement of the protein structure.

In the present study, $\bar{w} = 4$ is employed, providing a compromise that allows showing perturbations while maintaining the size of the IPN network small enough to exhibit fewer but stronger differences between the variants. A threshold $\bar{w} = 4$ (at least four atomic interactions gained or lost for a link to be in the PN) is reasonably conservative, considering that the average link weight in the WT TTR AAN is $< w_{i,j} >= 12.4$ with $std(w_{i,j}) = 10.3$, over a total of 1175 links.

3.5. Fiber model

Depending on the position of the candidate interface obtained through the IPN in the protein chain and on the relative position of the chains that build the quaternary structure of the protein, it is possible to understand whether the repetition of identical oligomers or identical sets of oligomers (repeating units), interacting through the candidate interface, allows the growth of a fiber without steric clashes. Figure 3 shows the schematics of two possible cases: on the left-hand side, a case where the repetition of identical oligomers leads to a fiber; on the right-hand side, a case where the repetition of identical oligomers leads to a steric clash. In the first case, the validity of the fiber model can be assessed by comparison of its diameter with some experimental evidence. In the second case, two explanations are possible: either the selected candidate interface is not the right choice, or the selected candidate interface is correct but the oligomer dissociates before the initiation of the fiber-forming process and no fiber model can be produced based on the sole knowledge of the oligomer's crystalline structure.

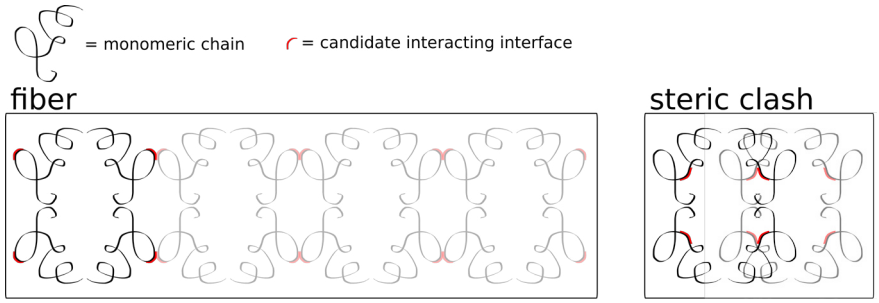

Fig. 3: Schematics of two possible cases of position of the candidate interacting interface in the protein oligomer. *Left:* a case where the repetition of identical oligomers leads to a fiber. *Right:* a case where the repetition of identical oligomers leads to a steric clash.

4. Results and Discussion

The cause of the increased tendency to amyloid fiber formation of the L55P TTR variant was investigated according to the following hypotheses:

1. A mutation allows the reproduction of the native structure if the AANs of the variant and of the WT have similar node properties (node degree k_i, node weight w_i and node's Neighborhood watch Nw_i) for all nodes i [20].
2. The dynamics of atoms in the variant are similar to the dynamics of atoms in the WT protein if the link weights w_{ij} are similar in the AANs of the variant and of the WT. The influence of link weights on the dynamics on networks has been proven for synthetic and real-word networks [24] and the relation between link weights in the AAN of a protein and its dynamics have been shown in previous work [21]. As mentioned in the Introduction, the atomic motions that can take place in a protein are determined by the protein structure: as a result, differences in atomic contacts, measured by differences in the link weights in the AAN, probe for a different encoding of the dynamics accessible by the atoms.

First, we verified the first hypothesis by comparing the node properties of the AANs of WT and L55P TTR. For comparison, we performed the same calculation for another pathogenic (V30M) and two non-pathogenic (T119Y and T119M) variant structures. The AANs of the WT, L55P, V30M, T119Y and T119M TTR variants share very similar node properties along the sequence (Appendix, Figure S1). This means that all the variants are capable of reproducing the TTR native structure, and that the pathogenicity of the L55P and V30M variants is related to their dynamics, different from the WT TTR. This is consistent with a low Root Mean Square Deviation between the variants' structure and the WT structure (RMSD values: 0.58 Å, 0.58 Å, 0.54 Å and 0.34 Å for L55P TTR, V30M TTR, T119Y TTR and T119M TTR, respectively, calculated with TopMatch [25]). It must be noted that the RMSD measure is performed considering only the position of the backbone atoms of the protein, while the comparison of the node degree k_i, node weight w_i and node's Neighborhood watch Nw_i for each amino acid in the AAN of the protein variant takes into consideration all atoms in the protein's structure (excluding hydrogen atoms since they are not detected by X-ray crystallography). As such, a similarity in node properties in the AAN is a stricter criterion to assess protein structures similarity. While a low value of RMSD means that the shape of the protein is conserved among two variants, all nodes having the same degree, weight and Neighborhood watch in the AAN of two protein variants means that the number of contacts, that is, the amino acid and atomic packing around each amino acid, is conserved. Nevertheless, an amino acid may have the same degree, weight and Neighborhood watch in the AAN of two protein variants but performing a different number of atomic contacts with its neighbors, resulting in a different link weight, if it moves closer to some neighbor(s) and further from other(s).

To test the second hypothesis, we employed IPNs to compare the link weights in the AAN of each variant with the ones of the AAN of the WT. We used IPNs instead of PNs to focus on the atomic motions and rearrangement of atomic contacts resulting from the mutation of the amino acid at the mutation site. The IPNs of the L55P, V30M, T119Y and T119M TTR variants are reported in Figure 4. Green links between nodes in the IPN mean that the corresponding

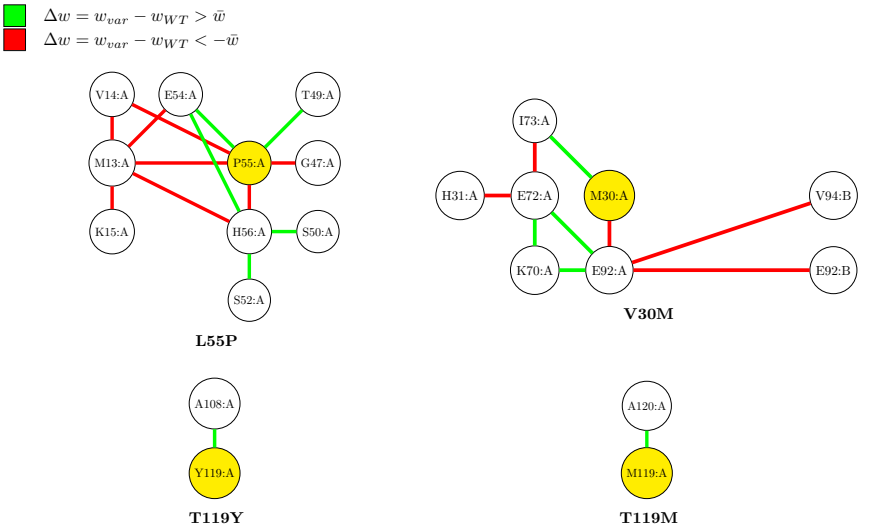

Fig. 4: Induced Perturbation Networks (threshold $\bar{w} = 4$) for four TTR variants. Green links between nodes in the IPN mean that the corresponding amino acids are closer in the variant's structure compared to the WT (more atomic interactions); viceversa, red links in the IPN mean that the two amino acids are further in the variant's structure compared to the WT.

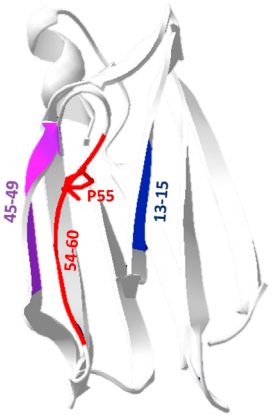

Fig. 5: TTR L55P variant: position of the candidate new interacting interface (in red). For clarity, only one chain is shown.

amino acids are closer in the variant's structure compared to the WT (more atomic interactions); on the contrary, red links in the IPN mean that the two amino acids are further in the variant's structure compared to the WT. The IPN of L55P (Figure 4, top left) shows the presence of both red and green links, showing that a complex rearrangement of atomic positions, leading to atomic interaction changes, has taken place due to the mutation with respect to the native structure. In contrast, the IPNs of the non-pathogenic variants T119Y and T119M (Figure 4, bottom) have only one green link. This means that the T119Y and T119M non-pathogenic mutations have a very mild impact on the atomic interactions in the protein structure. Finally, the IPN of another pathogenic variant (V30M, Figure 4, top right) shows the presence of both red and green links (as the L55P IPN, contrarily to the non-pathogenic variants' IPNs), different from the IPN of L55P. These results show how the IPNs of pathogenic variants have different IPNs compared to non-pathogenic variants. Moreover, the IPN allows recognizing differences among pathogenic variants (L55P and V30M), consistent with different fiber formation mechanisms for V30M and L55P TTR.

The IPN of L55P TTR (Figure 4, top left) shows that the loop containing residues S52 to E54 (red in Figure 5) looses interactions with the β-strand containing residues M13 to K15 (blue in Figure 5) and changes orientation angle with respect to the β-strand containing residues G47 to T49 (purple in Figure 5) since some atomic interactions are lost (red P55-G47 link) and some are gained (green P55-T49 link). Based on these observations, we made the hypothesis that the E54-T60 loop moves away from the rest of the structure, resulting from the loosening of atomic interactions with the M13, V14, K15 residues, and forms the new interacting interface that allows the fiber to grow (Figure 5).

The second pathogenic variant considered here, V30M, shows a different IPN compared to the IPN of the L55P TTR variant, suggesting that the pathways of fiber formation of these two variants are different. Contrary to the L55P mutation, the IPN of V30M (Figure 4, top-right panel) shows how the perturbation due to the single amino acid mutation in a chain of the TTR dimer reaches the second chain of the dimer: the nodes V94:B and E92:B are present in the IPN of V30M. Moreover, the links (E92:A, V94:B) and (E92:A, E92:B) that involve these nodes are red ($w_{V30M}(i,j) - w_{WT}(i,j) < -\bar{w}$), reflecting a loss of atomic interactions at the dimer interface due to the V30M mutation. This suggests that the V30M TTR tetramer probably dissociates to form the amyloid fiber, in agreement with the recent experimental analysis of the fibrils from a patient with V30M TTR amyloidosis [15].

The possibility for a specific segment to form the novel interface for the amyloid fiber growth depends on two factors: the spatial occupancy of the protein structure and the chemical affinity between two copies of the segment. In the

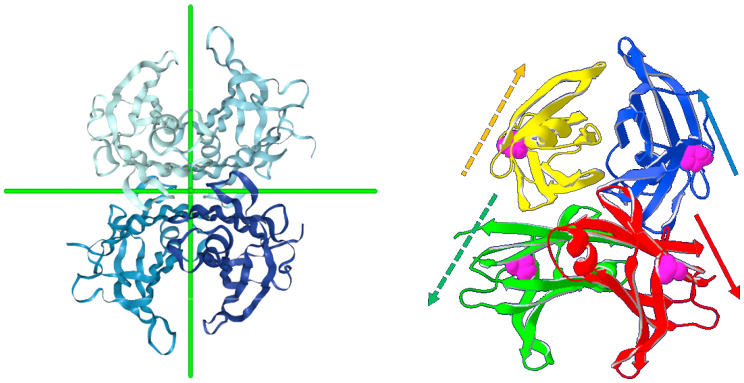

Fig. 6: Tetrameric structure of TTR. *Left*: dihedral symmetry axes of the tetramer. *Right*: position of the P55 residue in the L55P variant (in pink) and relative orientation of the candidate interacting interfaces on each chain (arrows).

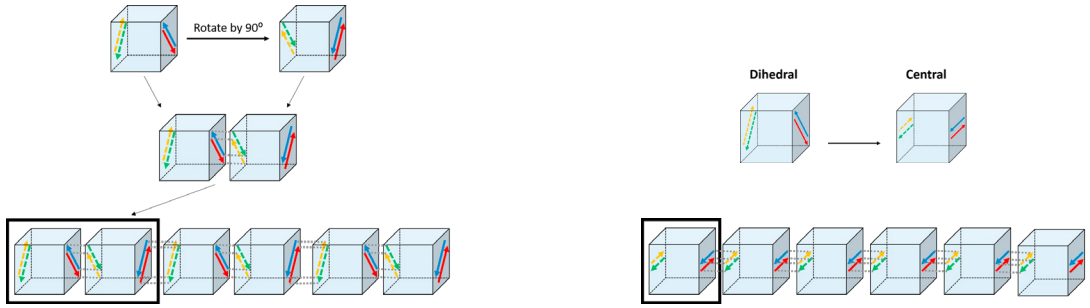

Fig. 7: Model for fibers resulting from the creation of an active interface (arrows) on each chain of a tetrameric protein with dihedral symmetry. (a) *Dihedral fiber* model. A tetramer with dihedral symmetry can interact with a copy of itself rotated by 90 degrees through the interaction interfaces (arrows). The obtained octamer (in the box) constitutes the repeating unit for a fiber model. (b) *Central fiber* model. If the interaction interfaces (arrows) of a tetramer with central symmetry are mobile enough, they can align with an axis of symmetry of the tetramer, degenerating to a central symmetry. The degenerated tetramer can interact with a copy of itself. The degenerated tetramer (in the box) constitutes the repeating unit for a fiber model.

following, we focus on the first aspect, to determine whether the candidate interface for the L55P TTR inferred from its IPN satisfies the first necessary criterion, that is, allowing the growth of a fiber-like structure, without producing steric clashes.

In order to understand whether the new candidate interface can allow the growth of an amyloid-like structure of repeating units of L55P TTR oligomers, the symmetry of the TTR tetramer was taken into consideration. The native TTR tetramer has a dihedral symmetry (Figure 6, left panel); as a consequence, the interacting interface on the four chains will follow the same symmetry if no dissociation of the tetramer happens (arrows in Figure 6, right panel). As schematized in Figure 7a, a tetramer with the interfaces following a dihedral symmetry will be able to interact with a copy of itself after a rotation of 90 degrees. Then, the obtained octamer will constitute a repeating unit for a tiling model, eventually resulting in an elongated fiber-like structure. In the following, we refer to a so-constructed fiber model as a *dihedral fiber model*. Alternatively, provided a sufficient mobility of the interfaces, they could align along a symmetry axis of the tetramer and degenerate to a central symmetry (Figure 7b, top). In this situation, the tetramer itself would represent the repeating unit for a tiling model, as schematized in Figure 7b (bottom). In the following, we refer to a so-constructed fiber model as a *central fiber model*. Figure 8 shows the *dihedral* and *central* fiber models for L55P TTR. Due to the geometry of the TTR oligomer, the *dihedral* model produces a fiber of diameter of around 69 Å, while the *central* model produces a fiber with an ellipsoidal cross-section, with a major axis of around 69 Å

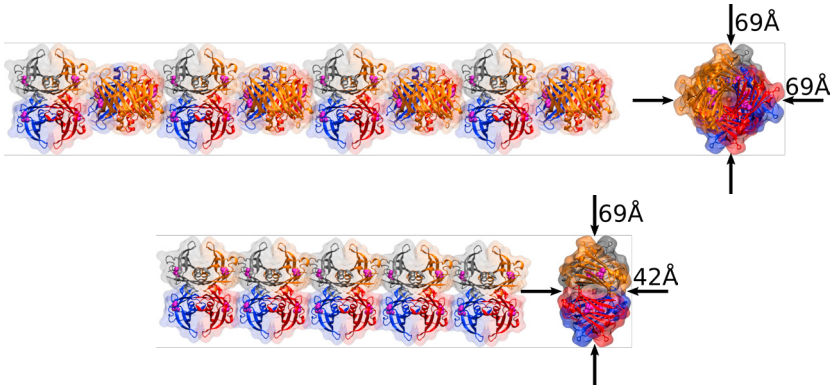

Fig. 8: Fiber models for the TTR L55P variant. *Top: Dihedral fiber* model. *Bottom: Central fiber* model.

and a minor axis of around 42 Å. Interestingly, a crystallographic study of L55P TTR (PDB id: 5ttr [26]) showed that the protein crystallized with the same symmetry as the the repeating unit of the *dihedral fiber model* proposed here. The observation of an asymmetric unit of this symmetry lead the authors of the study to propose that L55P exists in an amyloidogenic conformation, that would explain its higher propensity to the formation of amyloids compared to the WT. The *dihedral fiber model* perfectly matches the model proposed in reference [26], even though it was produced from a different crystalline structure and using different tools. Finally, electron micrographs of L55P TTR protofilaments produced *in vitro* show a diameter of 60 to 65 Å [27], consistent with the *dihedral fiber model*. The mentioned experimental evidences support the *dihedral fiber model* as a model for the amyloid fiber formed by the L55P TTR variant.

5. Conclusion

The analysis of the IPNs of TTR variants have shown how the IPN probes atomic motions and atomic links rearrangement that are consistent with the dynamics differences measured experimentally. As such, it represents a computationally-light tool to assess the differences in atomic interactions existing in the crystalline structure of protein variants that can lead to changes in the protein behavior: in the case of TTR, the change in propensity for amyloid formation. It is noticeable that few changes in atomic interactions (twelve links in the L55P TTR IPN over 228 amino acids in the TTR dimer and 1175 links in the WT TTR dimer AAN) can lead to a drastic change in the protein's dynamics. Moreover, we have presented a tiling model to account for the geometrical constraints underlying fiber formation, necessary for the validation of the candidate novel interacting interfaces extracted from the analysis of the IPN. The coupling of the IPN and the tiling model has allowed the construction of a fiber model for the L55P TTR variant, that satisfies the geometrical constraints imposed by the symmetry of the TTR tetramer structure and is in agreement with experimental results. The proposed model does not require the dissociation of the tetramer prior to fiber formation. The methodology used in this study relies on the sole knowledge of the X-ray structure of protein variants and takes into consideration the space occupancy of whole protein structure for the construction of fiber models. This is necessary to ensure that the proposed novel interacting interface does not produce steric clashes when the aggregation of entire proteins is modeled.

Acknowledgements

The authors thank the CNRS Interdisciplinary Mission (MITI) for funding (Défi OASIC-2017-2018, project GoPro).

Appendix A.

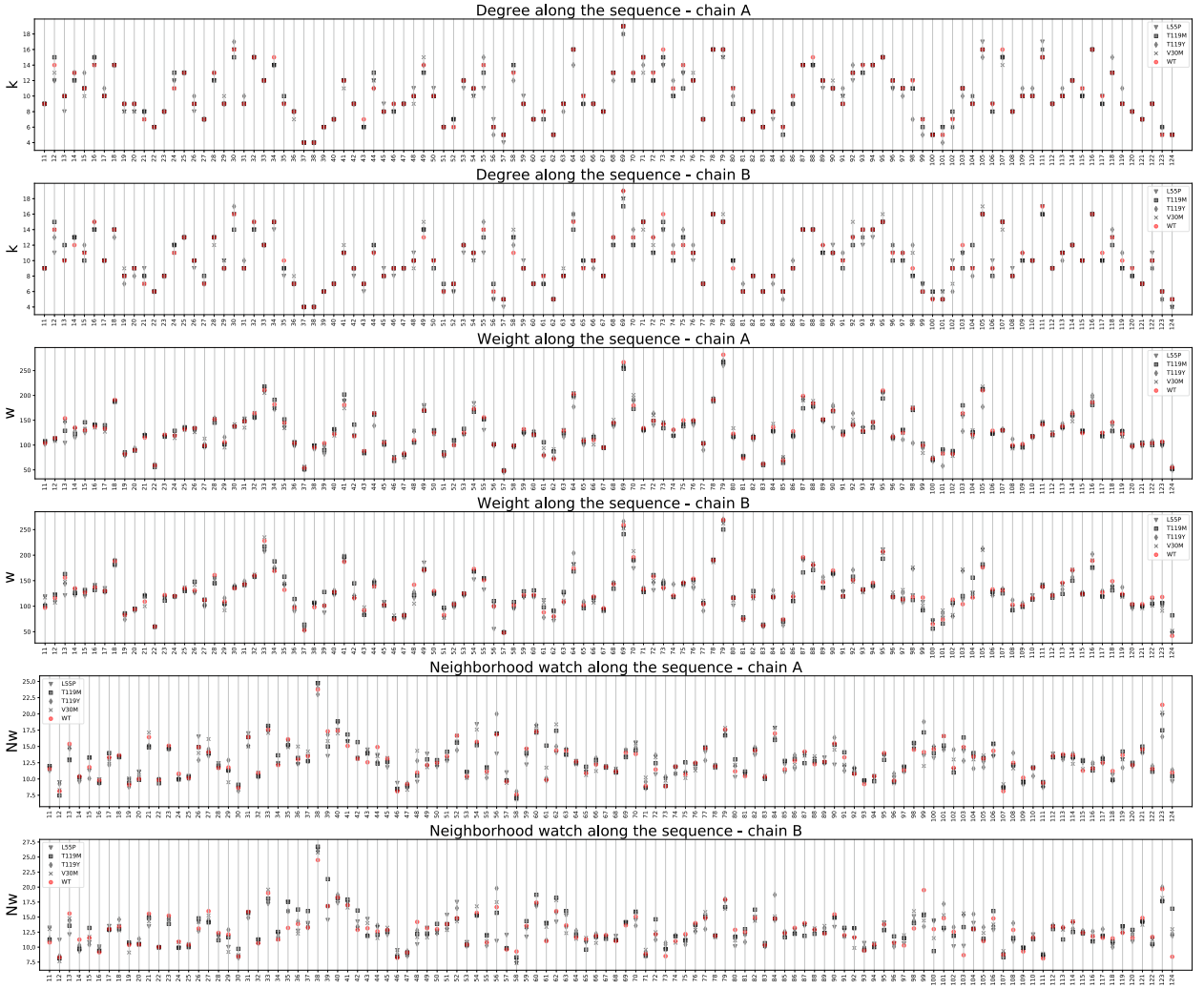

Fig. S1: Node properties (degree k, weight w and Neighborhood watch $Nw = w/k$) of the amino acids of the TTR variants in their Amino Acid Networks, along the protein amino acid sequence. From top to bottom: degree k (chain A), degree k (chain B), weight w (chain A), weight w (chain B), Neighborhood watch $Nw = w/k$ (chain A), Neighborhood watch $Nw = w/k$ (chain B).

References

[1] T. Haliloglu, I. Bahar, Adaptability of protein structures to enable functional interactions and evolutionary implications, Current opinion in structural biology 35 (2015) 17–23.

[2] R. Ramachandran, R. K. Tweten, A. E. Johnson, Membrane-dependent conformational changes initiate cholesterol-dependent cytolysin oligomerization and intersubunit β-strand alignment, Nature structural & molecular biology 11 (8) (2004) 697–705.

[3] L. Robert, J. Ollion, J. Robert, X. Song, I. Matic, M. Elez, Mutation dynamics and fitness effects followed in single cells, Science 359 (6381) (2018) 1283–1286.

[4] R. N. McLaughlin Jr, F. J. Poelwijk, A. Raman, W. S. Gosal, R. Ranganathan, The spatial architecture of protein function and adaptation, Nature 491 (7422) (2012) 138–142.

[5] J. Mercadier, How do mutations cause disease, Heart Metab 41 (2008) 34–37.

[6] F. Chiti, C. M. Dobson, Protein misfolding, amyloid formation, and human disease: a summary of progress over the last decade, Annual review of biochemistry 86 (2017) 27–68.
[7] M. J. M. Saraiva, Transthyretin mutations in hyperthyroxinemia and amyloid diseases, Human mutation 17 (6) (2001) 493–503.
[8] F. L. Ruberg, J. L. Berk, Transthyretin (ttr) cardiac amyloidosis, Circulation 126 (10) (2012) 1286–1300.
[9] L. Cendron, A. Trovato, F. Seno, C. Folli, B. Alfieri, G. Zanotti, R. Berni, Amyloidogenic potential of transthyretin variants insights from structural and computational analyses, Journal of Biological Chemistry 284 (38) (2009) 25832–25841.
[10] A. K. Dasari, R. M. Hughes, S. Wi, I. Hung, Z. Gan, J. W. Kelly, K. H. Lim, Transthyretin aggregation pathway toward the formation of distinct cytotoxic oligomers, Scientific reports 9 (1) (2019) 33.
[11] A. W. Yee, M. Aldeghi, M. P. Blakeley, A. Ostermann, P. J. Mas, M. Moulin, D. De Sanctis, M. W. Bowler, C. Mueller-Dieckmann, E. P. Mitchell, et al., A molecular mechanism for transthyretin amyloidogenesis, Nature communications 10 (1) (2019) 925.
[12] J. Hamilton, M. Benson, Transthyretin: a review from a structural perspective, Cellular and Molecular Life Sciences CMLS 58 (10) (2001) 1491–1521.
[13] A. K. Dasari, I. Hung, Z. Gan, K. H. Lim, Two distinct aggregation pathways in transthyretin misfolding and amyloid formation, Biochimica et Biophysica Acta (BBA) - Proteins and Proteomics 1867 (3) (2019) 344–349. doi:10.1016/j.bbapap.2018.10.013.
URL https://linkinghub.elsevier.com/retrieve/pii/S1570963918301882
[14] A. K. R. Dasari, I. Hung, B. Michael, Z. Gan, J. W. Kelly, L. H. Connors, R. G. Griffin, K. H. Lim, Structural Characterization of Cardiac Ex Vivo Transthyretin Amyloid: Insight into the Transthyretin Misfolding Pathway In Vivo, Biochemistry 59 (19) (2020) 1800–1803. doi:10.1021/acs.biochem.0c00091.
URL https://pubs.acs.org/doi/10.1021/acs.biochem.0c00091
[15] M. Schmidt, S. Wiese, V. Adak, J. Engler, S. Agarwal, G. Fritz, P. Westermark, M. Zacharias, M. Fndrich, Cryo-EM structure of a transthyretin-derived amyloid fibril from a patient with hereditary ATTR amyloidosis, Nature Communications 10 (1) (2019) 5008. doi:10.1038/s41467-019-13038-z.
URL http://www.nature.com/articles/s41467-019-13038-z
[16] C. Lesieur, L. Vuillon, From tilings to fibers–bio-mathematical aspects of fold plasticity, Oligomerization of Chemical and Biological Compounds (2014) 395.
[17] C. Lesieur, K. Schulten, Editorial overview: Theory and simulation, Current opinion in structural biology 31 (2015) vvi. doi:10.1016/j.sbi.2015.05.008.
URL https://doi.org/10.1016/j.sbi.2015.05.008
[18] J. R. Perilla, B. C. Goh, C. K. Cassidy, B. Liu, R. C. Bernardi, T. Rudack, H. Yu, Z. Wu, K. Schulten, Molecular dynamics simulations of large macromolecular complexes, Current opinion in structural biology 31 (2015) 64–74.
[19] L. Vuillon, C. Lesieur, From local to global changes in proteins: a network view, Current opinion in structural biology 31 (2015) 1–8.
[20] R. Dorantes-Gilardi, L. Bourgeat, L. Pacini, L. Vuillon, C. Lesieur, In proteins, the structural responses of a position to mutation rely on the goldilocks principle: not too many links, not too few, Physical Chemistry Chemical Physics 20 (39) (2018) 25399–25410.
[21] A. Gheeraert, L. Pacini, V. S. Batista, L. Vuillon, C. Lesieur, I. Rivalta, Exploring allosteric pathways of a v-type enzyme with dynamical perturbation networks, The Journal of Physical Chemistry B 123 (16) (2019) 3452–3461.
[22] A. Hagberg, P. Swart, D. S Chult, Exploring network structure, dynamics, and function using networkx, Tech. rep., Los Alamos National Lab.(LANL), Los Alamos, NM (United States) (2008).
[23] M. Bastian, S. Heymann, M. Jacomy, Gephi: an open source software for exploring and manipulating networks, in: Third international AAAI conference on weblogs and social media, 2009.
[24] S. Unicomb, G. Iñiguez, M. Karsai, Threshold driven contagion on weighted networks, Scientific reports 8 (1) (2018) 1–10.
[25] M. J. Sippl, M. Wiederstein, Detection of Spatial Correlations in Protein Structures and Molecular Complexes, Structure 20 (4) (2012) 718–728. arXiv:22483118, doi:10.1016/j.str.2012.01.024.
URL https://www.cell.com/structure/abstract/S0969-2126(12)00055-X
[26] M. P. Sebastião, M. J. Saraiva, A. M. Damas, The crystal structure of amyloidogenic leu55 pro transthyretin variant reveals a possible pathway for transthyretin polymerization into amyloid fibrils, Journal of Biological Chemistry 273 (38) (1998) 24715–24722.
[27] H. A. Lashuel, C. Wurth, L. Woo, J. W. Kelly, The most pathogenic transthyretin variant, l55p, forms amyloid fibrils under acidic conditions and protofilaments under physiological conditions, Biochemistry 38 (41) (1999) 13560–13573.